IEEE Trans on Antennas and Propagation, 2016, 64:1, pp. 335-360, DOI: 10.1109/TAP.2015.2501844

Single-Feed Ultra-Wideband Circularly Polarized Antenna with Enhanced Front-to-Back Ratio

Long Zhang, Steven Gao, Qi Luo, Paul R. Young, Qingxia Li, Youling Geng and Raed A. Abd-Alhameed

Abstract—**This communication presents a single-feed ultra-wideband circularly polarized (CP) antenna with high front-to-back ratio (FBR). The antenna is composed of two orthogonally placed elliptical dipoles printed on both sides of a substrate. To realize high front-to-back ratio, a novel composite cavity is also proposed and integrated with the presented crossed dipoles, which effectively reduces the back-lobe of the crossed dipoles. Simulation results are in good agreement with measured results which demonstrate an impedance bandwidth from 0.9 to 2.95GHz (106.5%) and a 3-dB axial ratio bandwidth from 1 to 2.87GHz (96.6%). The measured FBR is about 30dB across the whole GNSS band. Compared with other reported single-feed wideband CP antennas, the antenna has advantages such as a wider CP bandwidth and lower back-lobe radiation.**

Index Terms—**Crossed dipoles, single-feed antennas, circular polarization, wideband antenna, back-lobe reduction.**

I. Introduction

CIRCULARLY polarized antennas are widely used in global navigation satellite systems (GNSS), RFID, satellite communication systems and wireless power transmission systems due to their capabilities of reducing polarization mismatch and suppressing multipath interferences [1].

Generally, the CP antennas can be divided into two categories, single-feed and multi-feed. With the trend of increasing capacity of various wireless communication systems, the bandwidth of CP antennas needs to be enhanced. However, it is always challenging to design a broadband CP antenna with single feed. One type of single-feed broadband CP antenna is the spiral antenna. However, their bi-directional radiation properties make these conventional spiral antennas unsuitable for some applications such as GNSS application since a directional radiation pattern is needed to decrease the effects of the reflections from the ground [2]. Several directional spiral antennas including spiral-mode microstrip antenna (SMM) [3], conducting plane backed spiral [4] and cavity backed spiral [5] have been proposed to conquer this problem. Another issue of the spiral antennas is the need for a balun, which increases the complexity of the spirals.

Recently, a single-feed crossed dipole with integrated phase delay line was presented in [6]. This antenna can achieve more than 15% 3-dB axial ratio (AR) bandwidth with a simple feeding structure. To enhance the bandwidth, parasitic loops are introduced and a 28.6% CP bandwidth is achieved [7]. By using rectangular patches instead of linear dipoles, a 27% 3-dB AR bandwidth can be attained [8].

Since the crossed dipole antenna radiates in bi-direction [9], flat ground planes [6-8] and metallic cavities [10, 11] are adopted to decrease the back radiation and enhance the FBR. The FBR is about 15dB in [6, 7] and 10dB in [8] when a flat ground plane is used. When cavities are utilized to reduce the back radiation further, the FBR can go up to 25dB at several frequency points [10, 11]. Considering that the antennas in [10, 11] are multi-band CP antennas, it is not clear whether these cavities can achieve high FBR in a broadband frequency range.

In this communication, an ultra-wideband CP antenna is presented. It is able to cover all GNSS frequency bands and a part of S-band. To enhance the FBR of this antenna, a novel composite cavity with unequal-length crossed fins is designed and then integrated with the antenna. Measurement results indicate that the proposed ultra-wideband CP antenna can work from 1GHz to 2.87GHz while maintaining very low back-lobe level across the whole GNSS band. Compared with other CP crossed dipole antennas [6-11], the proposed antenna has much wider CP bandwidth and higher FBR in a broadband frequency range.

II. Antenna Geometry and Cavity Design

In this section, the antenna configuration will be given at first and then a composite cavity for improving the FBR of the proposed antenna is proposed. The design concept of the composite cavity and the comparison with other types of cavity are also presented.

A. Antenna Geometry

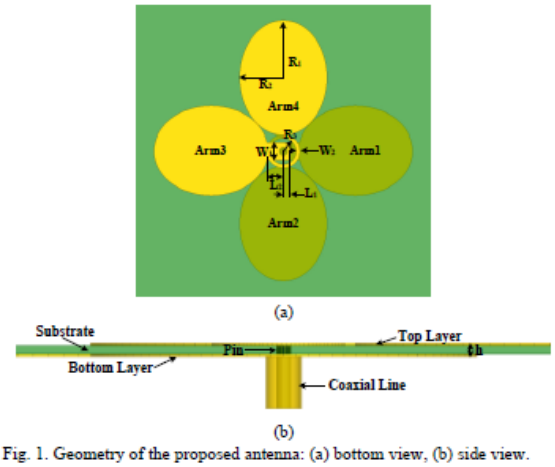

Fig. 1. Geometry of the proposed antenna: (a) bottom view, (b) side view.

Fig. 1 shows the configuration of the proposed single-feed ultra-wideband CP antenna. The antenna consists of two pairs of double-sided elliptical dipoles which are placed perpendicular to each other. The dipole arm 1 & 2 and 3 & 4 are both connected by ring-shaped phase delay lines, which introduce a 90° phase difference between the orthogonally

Manuscript received March 13, 2015.

L. Zhang, S. Gao, Q. Luo and P. R. Young are with the School of Engineering and Digital Arts, University of Kent, Canterbury CT2 7NT, UK. (emails: lz76@kent.ac.uk; s.gao@kent.ac.uk; qiluo@ieee.org; p.r.young@kent.ac.uk).

Q. Li is with the School of Electronic Information and Communications, Huazhong University of Science and Technology, Wuhan 430074, China.

Y. L. Geng is with Hangzhou Dianzi University, China.

R. A. Abd-Alhameed is with the University of Bradford, U.K.

placed dipole pairs to produce circularly polarized radiation.

The antenna is etched on a 0.817 mm thick Rogers RO4003C substrate with a relative permittivity of 3.55 and a loss tangent of 0.0027. The four elliptical dipole arms are all characterized by a major axis length R_1 and minor axis length R_2 while the phase delay line is a 3/4 ring with inner radius R_3 and line width W_2. A pair of partly overlapped rectangular patches with width W_1 are printed on both sides of the substrate and are used for placing the coaxial feed line. Furthermore, the patches are employed to tune the impedance matching of the proposed antenna by introducing proper capacitance.

Similar to conventional crossed dipole CP antenna, the proposed antenna radiates in bi-direction. As shown in Fig. 1, current phase on arm 1 is ahead of current phase on arm 2 and thus a RHCP wave is excited along broadside direction while a LHCP wave propagates along downward direction.

The antenna geometry parameters are shown in TABLE I.

TABLE I
ANTENNA PARAMETERS (MM)

W_1	W_2	R_1	R_2	R_3	h	L_1	L_2
7.5	1.5	23.4	18	5.2	0.817	2.5	6.2

B. Cavity Design Concept

To improve the FBR of the proposed antenna, a novel composite cavity is proposed and shown in Fig. 2. It can be seen from Fig. 2 that it is composed of a cylindrical cavity with crossed unequal length fins. The composite cavity is designed in such a way to reduce the back-lobe of the antenna maximally.

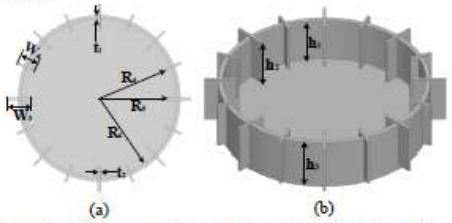

Fig. 2. Geometry of the proposed composite cavity: (a) top view, (b) prospective view.

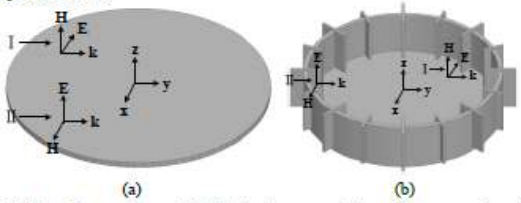

Fig. 3. Two plane waves on: (a) flat circular ground plane, (b) proposed cavity.

It is well known that the surface wave propagating along the ground plane reradiates at the ground plane edge and thus increase the side-lobes as well as the back-lobe of the antenna. Therefore, suppressing the propagation of surface waves can reduce the back-lobe of the antenna. To explain the working mechanism of the proposed composite cavity in terms of surface wave suppression, similar analysis methods to [2, 12] are adopted.

Considering the two TEM plane waves Ⅰ and Ⅱ shown in Fig. 3, they can be denoted by the following equations respectively.

$$E_x(y,t) = E_{x0}\cos(ky - \omega t + \varphi_1) \quad (1)$$

$$E_z(y,t) = E_{z0}\cos(ky - \omega t + \varphi_2) \quad (2)$$

The boundary condition of flat conductor ground plane imposes that no tangential electric field can exist, i.e.

$$E_t = 0 \quad (3)$$

This equation indicates that plane wave Ⅰ cannot propagate along the circular ground plane while wave Ⅱ can exist. Considering the situation in Fig. 3 (b), wave Ⅰ cannot propagate along the cavity bottom due to the boundary condition given by equation (3). In contrast to the flat circular ground plane, wave Ⅱ cannot propagate along the proposed cavity either since there is a mandatory boundary condition imposed by the vertical cylindrical wall as well as the crossed fins. Therefore, it can be expected that the proposed composite cavity can offer better ability of surface wave suppression compared to regular circular flat ground plane.

As indicated above, the proposed antenna radiates in bi-direction, RHCP towards the broadside and LHCP backward. Conventionally, a large ground plane or a cavity is required to reduce the back-lobe of such kinds of antenna by reflecting the downward waves into the upward direction [7, 10]. The proposed composite cavity placed underneath the antenna shows better back-lobe reduction ability by minimizing diffracted waves; the mechanism can be explained as follows.

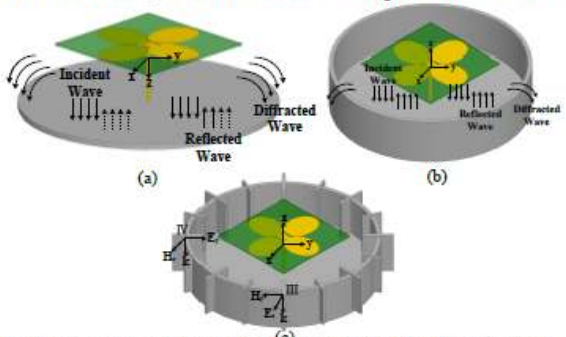

Fig. 4. Downward wave above: (a) flat circular ground plane, (b) cylindrical cavity, (c) the proposed composite cavity.

Fig. 4 depicts the propagation of downward LHCP wave excited by the antenna under different situations. When the proposed antenna is placed above a large flat ground plane, the majority of the LHCP wave will be reflected by the ground plane. However, considerable downward waves can still propagate across the ground plane due to the diffraction of these waves and result in large back-lobe. This diffraction effect can be decreased by replacing the flat ground plane with a cylindrical cavity shown in Fig. 4 (b) as the peripheral vertical wall can stop part of the diffracted waves.

A LHCP wave depicted in Fig. 4 can be expressed by the following equation.

$$\vec{E}(z,t) = \overrightarrow{E_x}\cos(-kz - \omega t + \pi/2) + \overrightarrow{E_y}\cos(-kz - \omega t) \quad (4)$$

where $|\overrightarrow{E_x}| = |\overrightarrow{E_y}|$.

As a circularly polarized wave, the electric field vector $\vec{E}$ rotates on xy plane. To analyze the downward wave around the

peripheral wall of the proposed composite cavity, two transient plane waves Ⅲ and Ⅳ whose electric field are along the $+x$ and $+y$ direction, respectively, are plotted in Fig. 4 (c). These two waves cannot propagate along the vertical fins due to the boundary condition given by equation (3). Actually all the 16 vertical fins can be used to block the diffracted waves when the direction of the transient E vector is parallel to these fins. Therefore, the proposed cavity is more advantageous for back-lobe reduction than the regular cylindrical cavity.

C. Comparison of Back-lobe Reduction

It has been shown that the proposed composite cavity can offer better back-lobe reduction ability than a flat ground plane and regular cylindrical cavity. This performance enhancement is mainly from the suppression of surface waves and the blocking of diffracted waves around the edge of the ground plane. To verify this analysis, a comparison between a flat plane ground, regular cylindrical cavity and the proposed composite cavity, in terms of the back-lobe reduction, is given.

The geometry dimensions of proposed composite cavity are given in TABLE II.

TABLE II
COMPOSITE CAVITY DIMENSIONS (MM)

W_3	W_4	R_4	R_5	R_6	h_1	h_2	h_3	t_1	t_2
35	25	100	95	110	50	52	55	5	3

For the flat ground plane and regular cylindrical cavity, the most critical dimensions for back-lobe reduction are the ground plane size as well as the height from antenna to ground plane. To make an unprejudiced and reasonable comparison, the proposed antenna in section Ⅱ is placed at a height of $h_1 = 50$ mm to the ground plane for all the three cases. Meanwhile, the radius of the ground plane is kept as 110mm.

The simulated back-lobe levels for the three ground plane reflectors are shown in Fig. 5. As shown in this figure, the back-lobe is very high when a flat ground plane is employed. By using the regular cylindrical cavity, back-lobes smaller than -12 dB can be achieved across the whole GNSS band. Further back-lobe reduction has been observed through utilizing the proposed composite cavity. It can be noted that about 2dB and more than 5 dB enhancement in back-lobe reduction can be achieved below and above 1.6GHz, respectively, when compared to cylindrical cavity backed antenna.

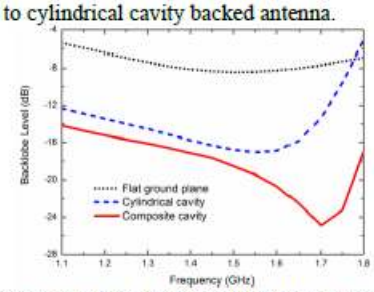

Fig. 5. Comparison of back-lobe level using different ground plane reflectors.

D. Cavity Optimization

The cavity dimensions such as the length of fins and the radius of the cavity play an important role in back-lobe reduction. Fig. 6 depicts the back-lobe level and antenna gain under different pairs of W_3 and W_4. As indicated in this figure, the antenna gain under three states is similar. Under equal-length fins, the back-lobe degrades when the fins length increase. The back-lobe level under unequal-length fins state is similar to the equal 25mm fins situation across the GNSS band. However, the latter case features a sharp increase in back-lobe level in higher frequency and thus the unequal-length fins are chosen.

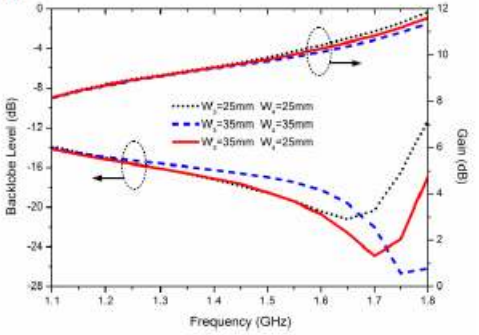

Fig. 6. Back-lobe level and antenna gain under different W_3 and W_4.

It is shown in Fig. 7 that the antenna gain increases with larger cavity radius. However, the back-lobe increases after exceeding 1.5GHz when R_6 is 120mm. Since the aim is to keep low back-lobe radiation across the GNSS band, the cavity radius R_6 is therefore to be kept at 110mm.

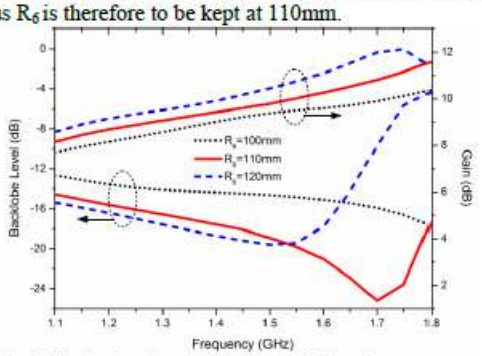

Fig. 7. Back-lobe level and antenna gain under different R_6.

III. RESULTS AND ANALYSIS

In this section, the simulated and measured results including the VSWR, AR, radiation pattern and antenna gain of the proposed antenna are given to verify its performance.

A. VSWR

The prototype of the proposed ultra-wideband composite cavity backed CP antenna is shown in Fig. 8.

The simulated and measured VSWRs of the proposed antenna are shown in Fig. 8. As can be seen from this figure, the measured VSWR is in good agreement with the simulated one. The simulated and measured results both indicate a 0.9 GHz to 2.95 GHz (3.28:1=106.5%) impedance bandwidth can be achieved by the proposed antenna.

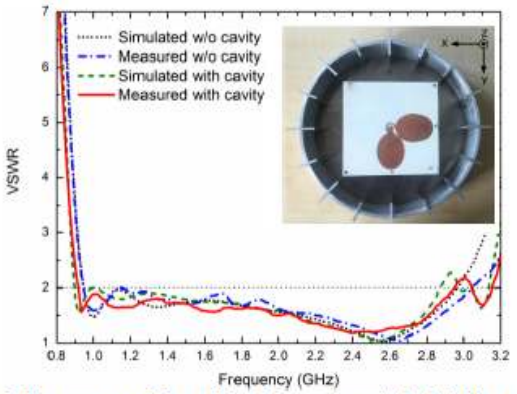

Fig. 8. The prototype of ultra-wideband composite cavity backed CP antenna and VSWR of the proposed antenna with and without cavity.

B. *Axial Ratio*

To evaluate the CP performance of the proposed antenna, the AR characteristics versus frequency relationship is given in Fig. 9. As shown in the figure, the measured 3dB AR bandwidth with cavity is from 1 GHz to 2.87 GHz (2.87:1=96.6%), which can cover the whole GNSS bands and a part of S band.

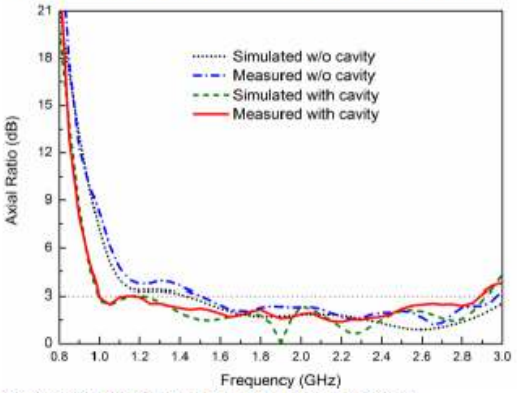

Fig. 9. Simulated and measured AR of the proposed antenna.

C. *Radiation Pattern and Gain*

The radiation pattern of the proposed antenna is measured using a linearly polarized horn antenna and the method presented in [13] is employed to get RHCP and LHCP radiation patterns.

Fig. 10 shows the radiation patterns of the proposed ultra-wideband CP antenna in two main planes (XoZ and YoZ planes) at 1.1 GHz, 1.4 GHz, 1.7 GHz and 2. 4GHz.

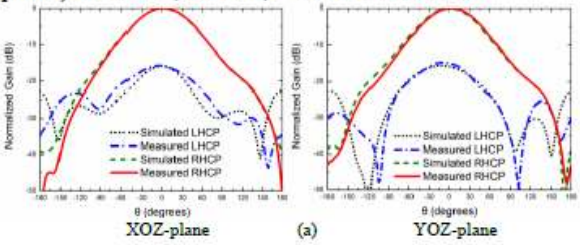

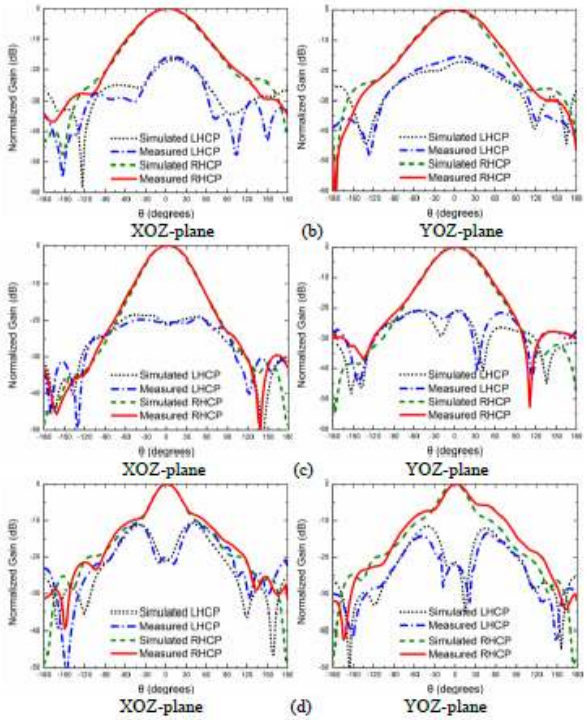

Fig. 10. Simulated and measured radiation patterns at: (a) 1.1GHz, (b) 1.4GHz, (c) 1.7GHz, (d) 2.4GHz.

As shown in the figure, the proposed antenna can achieve larger than 30dB FBR across the whole GNSS frequency band. The 3dB AR beamwidth is about 129° (XoZ plane) and 120° (YoZ plane) at 1.1GHz, 156° (XoZ plane) and 63° (YoZ plane) at 1.4GHz, 66 ° (XoZ plane) and 84° (YoZ plane) at 1.7 GHz.

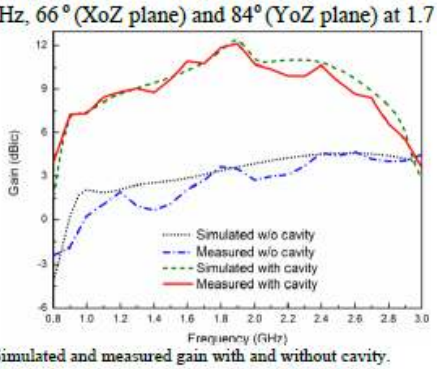

Fig. 11. Simulated and measured gain with and without cavity.

Fig. 11 shows the simulated and measured gain with and without cavity integrated. As shown in the figure, the antenna gain is around 9dBi when the cavity is employed, which also indicates an average 6dB gain enhancement is achieved compared with the results measured from the antenna only. The difference between the measured and simulated results may term from the measurement errors.

D. *Analysis of the CP Characteristic*

To investigate the ultra-wideband CP characteristic of the proposed antenna, the electric field distributions above the

aperture at 1 GHz, 1.8 GHz and 2.6 GHz are given in Fig. 12.

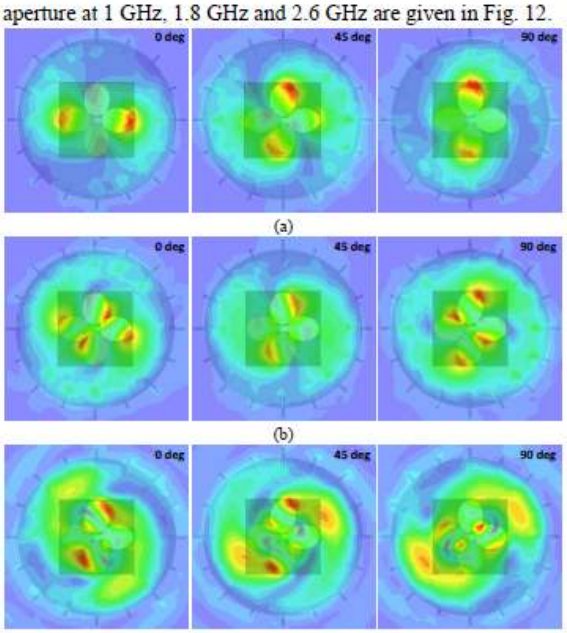

Fig. 12. Electric field distribution in the cavity aperture at different frequencies: (a) 1GHz, (b) 1.8GHz, (c) 2.6GHz.

As can be seen from the figure, the distribution of electric field is varied at different frequencies. From Fig. 12 (a), it can be noticed that the maximum electric field at phase angle 0° and 90° generate at the end of elliptical dipole arm. This indicates that the proposed antenna works at a half-wavelength dipole mode at 1 GHz. When the frequency increases to 1.8 GHz, the strongest electric field occurs at the side edge of the elliptical dipole arm. Therefore, it can be concluded that the resonance length of proposed antenna is decreased, which makes the antenna work at higher frequency band. At 2.6 GHz, the strong electric field no longer appears just around the antenna (see phase angle 90° in Fig. 12 (c)) and there are evident strong fields between the antenna and the cavity. Comparing this field distribution with those at lower frequencies, it is found that a higher mode is excited, which results in the deterioration of radiation pattern shown in Fig. 10 (d).

From the different electric field distributions at phase angle 0°, 45° and 90° in Fig. 12, it can be seen that a right-hand rotated electric field has been produced at all given frequencies. This indicates that the antenna can work as a circularly polarized antenna in an ultra-wideband frequency range.

In addition, the electric fields are almost all bounded by the cavity and little fields can propagate over the cavity as shown in Fig. 12 (a) and (b). This phenomenon verifies the back-lobe reduction ability of proposed antenna, which has been analyzed in section Ⅱ.

E. Comparison with Other CP Crossed Dipoles

TABLE III gives a comparison between the proposed antenna and other CP crossed dipoles in terms of impedance bandwidth, 3-dB AR bandwidth and average FBR. From this table, it can be seen that the proposed antenna has much wider CP bandwidth (3-4 times wider) and larger FBR compared with other reported CP crossed dipole antennas.

TABLE III
COMPARISON OF CP CROSSED DIPOLE ANTENNAS

Ref. No.	Impedance Bandwidth	3-dB AR Bandwidth	Average FBR
[6]	30.7%	15.6%	15dB
[7]	38.2%	28.6%	15dB
[8]	50.2%	27%	<10dB
[9]	11.8%	3.3%	-
This Paper	106.5%	96.6%	30dB

IV. CONCLUSION

A single-feed ultra-wideband circularly polarized antenna is proposed and investigated in this paper. To enhance the FBR, a novel composite cavity is deployed. The proposed antenna has a CP bandwidth of 96.6% and an average 30dB FBR across the GNSS band, which make the antenna very promising for wideband wireless systems.

REFERENCES

[1] S. Gao, Q. Luo, and F. Zhu, *Circularly polarized antennas*: John Wiley & Sons, 2013.
[2] F. Scire-Scappuzzo and S. N. Makarov, "A low-multipath wideband GPS antenna with cutoff or non-cutoff corrugated ground plane," *IEEE Trans. Antennas Propag.*, vol. 57, pp. 33-46, 2009.
[3] J. J. Wang and V. K. Tripp, "Design of multioctave spiral-mode microstrip antennas," *IEEE Trans. Antennas Propag.*, vol. 39, pp. 332-335, 1991.
[4] H. Nakano, *et al.*, "A spiral antenna backed by a conducting plane reflector," *IEEE Trans. Antennas Propag.*, vol. 34, pp. 791-796, 1986.
[5] H. Nakano, H. Oyanagi, and J. Yamauchi, "A wideband circularly polarized conical beam from a two-arm spiral antenna excited in phase," *IEEE Trans. Antennas Propag.*, vol. 59, pp. 3518-3525, 2011.
[6] J.-W. Baik, *et al.*, "Circularly polarised printed crossed dipole antennas with broadband axial ratio," *Electron. Lett.*, vol. 44, pp. 785-786, 2008.
[7] J.-W. Baik, T.-H. Lee, and e. al., "Broadband circularly polarized crossed dipole with parasitic loop resonators and its arrays," *IEEE Trans. Antennas Propag.*, vol. 59, pp. 80-88, 2011.
[8] Y. He, W. He, and H. Wong, "A wideband circularly polarized cross-dipole antenna," *IEEE Antennas Wireless Propag. Lett.*, vol. 13, pp. 67-70, 2014.
[9] Y.-F. Lin, *et al.*, "Circularly polarized crossed dipole antenna with phase delay lines for RFID handheld reader," *IEEE Trans. Antennas Propag.*, vol. 60, pp. 1221-1227, 2012.
[10] S. Ta, *et al.*, "Multi-band, wide-beam, circularly polarized, crossed, asymmetrically barbed dipole antennas for GPS applications," *IEEE Trans. Antennas Propag.*, vol. 61, pp. 5771-5775, 2013.
[11] K. Saurav, D. Sarkar, and K. V. Srivastava, "Dual-Band Circularly Polarized Cavity-Backed Crossed-Dipole Antennas," *IEEE Antennas Wireless Propag. Lett.*, vol. 14, pp. 52-55, 2015.
[12] M. Maqsood, *et al.*, "A Compact Multipath Mitigating Ground Plane for Multiband GNSS Antennas," *IEEE Trans. Antennas Propag.*, vol. 61, pp. 2775-2782, 2013.
[13] B. Y. Toh, R. Cahill, and V. F. Fusco, "Understanding and measuring circular polarization," *IEEE Trans. Education*, vol. 46, pp. 313-318, 2003.